Investigation of the homogeneity of the distribution of sunscreen formulations on the human skin: characterization and comparison of two different methods

Alexa Teichmann
Charité-Universitätsmedizin Berlin
Department of Dermatology
Center of Experimental and Applied Cutaneous Physiology
Schumannstr. 20/21
10098 Berlin, Germany

Marc Pissavini
Louis Ferrero
Adeline Dehais
Leonhard Zastrow
Coty Inc.
International R&D Center Monaco
MC98000 Monaco

Heike Richter
Jürgen Lademann
Charité-Universitätsmedizin Berlin
Department of Dermatology
Center of Experimental and Applied Cutaneous Physiology
Schumannstr. 20/21
10098 Berlin, Germany

Abstract. The efficacy of sun protection, mostly realized by the application of sunscreen formulations, is commonly described by the sun protection factor (SPF). Previous investigations have shown that the efficacy of the sun protection *inter alia* depends on the homogeneity of the distribution of the topically applied sunscreen formulation on the human skin. Therefore, suitable methods are required to determine the homogeneity of topically applied substances on the skin surface. This study provides and compares two different methods, which enable this determination. Laser scanning microscopy allows the analysis of tape strips removed from skin treated with a sunscreen. These reflect the inhomogeneous distribution on the skin that can complementary be determined directly, utilizing a dermatological laser scanning microscope. For the second method, a chromatic confocal setup was utilized, which enables the study of the microtopography of skin replicas before and after the application of a sunscreen product. The two methods were applied for the evaluation of three different sunscreen formulations for each method. A correlation of the homogeneity of distribution with the *in vivo* SPF could be confirmed. Both methods are suitable to investigate the homogeneity of the tested sunscreen formulations, although they provide different advantages and disadvantages.
[DOI: 10.1117/1.2409291]

Keywords: sun protection factor; sun protection; laser scanning microscopy; microtopography; high resolution sensor; skin replica.

Paper 05380RR received Dec. 18, 2005; revised manuscript received Jun. 21, 2006; accepted for publication Jul. 5, 2006; published online Dec. 28, 2006.

1 Introduction

Sun protection represents a current topic, particularly, because UV irradiation has been correlated to the incidence of skin cancer and also skin aging.[1–3] Several measures to perform sun protection are available, such as avoiding the sun, using sunscreen, wearing a hat, wearing sunglasses, covering up, avoiding artificial tanning, and checking the skin regularly.[4] The application of sunscreen formulations represents a very suitable and commonly used measure to protect the skin, although the determination of the efficacy of sunscreens, mostly described by the sun protection factor (SPF), is still vehemently being debated. The traditional SPF measures the sun protection mainly for the UVB range by quantifying a biological response of the skin, the formation of the erythema. However, there are other known UV-induced skin damages, such as immune suppression, skin aging, and cancer formation.[5] Furthermore, for ethical reasons, it is questionable whether the skin of numerous volunteers should be harmed in order to identify the SPF of new UV filter substances. Therefore, several promising approaches have been made to develop methods to determine SPF *in vitro* or *ex vivo*, which covers the full solar UV spectrum.[6,7]

However, the SPF and the efficacy of sunscreens also depend, to a large extent, on the distribution of the sunscreen on the skin.[8–10] Investigations have shown that SPF values determined *in vivo* are considerably less than the values determined *in vitro* by UV absorption of sunscreens diluted in alcoholic solutions,[11–13] which is probably *inter alia* caused by inhomogeneous distribution of the sunscreen formulation due to furrows and wrinkles on the human skin.[14] Lademann et al.[14] investigated the influence of homogeneity of the distribution of UV filter substances on SPF. They found a difference in SPF up to one order of magnitude when the sunscreen was solved and therefore distributed homogeneously. Further approaches to treat this phenomenon were proposed using different calculation models to predict realistic SPFs.[9,11,15,16]

Address all Correspondence to: Alexa Teichmann, Charité-Universitätsmedizin Berlin, Department of Dermatology, Center of Experimental and Applied Cutaneous Physiology, Schumannstr. 20/21, 10117 Berlin, Germany; Tel.:+49 30 450 518 106; Fax:+49 30 450 518 918; E-mail: alexa.teichmann@charite.de.

1083-3668/2006/11(6)/064005/8/$22.00 © 2006 SPIE

Obviously, a direct correlation of homogeneity in the distribution of sunscreen formulations with the SPF exists, which offers the possibility to increase the SPF by optimizing the formulation and the filter substances,[14] as the distribution depends on both the properties of the formulations and on the filter substances. Therefore, a suitable analytical technique is required to analyze the distribution of topically applied sunscreens *in vivo* or *ex vivo*. Schulz et al. [8] utilized electron microscopy visualization and light microscopic investigations to study the distribution of three different types of titanium dioxide. A disadvantage of this method is that the removal of several punch biopsies is necessary, which represents a maximal invasive method for the volunteers. Lademann et al. [14] introduced laser scanning microscopy to visualize the distribution of a topically applied sunscreen both *in vivo*, directly on the skin surface, and *ex vivo* on tape strips that were removed from pretreated skin areas. A similar nonhomogeneous distribution was observed in both cases.

In the present study, this appropriate method described by Lademann et al. [14] was compared to a new optical method analyzing skin replica, concerning the microtopography and surface roughness before and after the application of different sunscreen formulations. The subtraction of both outcomes permits the study of the formulation distribution qualitatively and quantitatively.

2 Material and Methods

2.1 *Formulations*

Three different formulations were submitted by Lancaster (Monaco) for investigation by laser scanning microscopy and microtopography measurements. These sunscreens, A, B, and C, are based on emulsifier-free formulas (oil in water gel emulsion, Lancaster proprietary). Formulas A and B contain 30% of nonvolatile material (material left on skin after water evaporation). Formula C contains only 18% of nonvolatile material. The three sunscreens are composed of chemical UVB and UVA filters.

The *in vivo* determination of the SPF was carried out using the COLIPA (The European Cosmetic Toiletry and Perfumery Association) method.[17]

- Product A: sunscreen, SPF $in\,vivo = 14 \pm 4$ (COLIPA method, 5 volunteers)
- Product B: sunscreen, SPF $in\,vivo = 11 \pm 3$ (COLIPA method, 5 volunteers)
- Product C: sunscreen, SPF $in\,vivo = 6 \pm 1$ (COLIPA method, 5 volunteers)

0.1% fluorescein was added as a marker to the sunscreen formulations for visual determination of the distribution. In preliminary experiments, it was shown that the distribution of the UV filter substances was comparable to the distribution of the sodium fluorescein in the sunscreen formulation.

2.2 *SPF Simulation*

In vivo SPF values were compared to expected SPF values. These calculated values were simulated by a mathematical model taking into account the amount of UV filters present in the sunscreen products and for the amount deposited. This model, based on a continuous thickness distribution, has already been described by Ferrero et al.[9]

In the model, local film thickness (FT), h, was normalized as a fraction of local absolute FT to average FT. Thickness fraction h can be considered as being the inverse function of any relevant cumulative thickness distribution F. In our approach, F is considered as a variable ranging from 0 to 1 and $h_{(F)}$ is the inverse thickness distribution function.

The total transmittance $(Ts)_\lambda$ of the continuous sunscreen film was calculated at each wavelength, by integrating the following equation along variable F

$$(Ts)_\lambda = \int_0^1 10^{-h_{(F)}A\lambda} \mathrm{d}F. \tag{1}$$

A_λ is the absorbance of the uniform average film characterized by a unique thickness fraction $h=1$. A_λ was calculated at wavelength λ, applying the Beer-Lambert law to the sunscreen's UV filter composition, which was deposited at 2 $\mathrm{mg/cm^2}$.

Among the different available inverse thickness distribution functions $h_{(F)}$, one was found to be highly relevant: the gamma law, which is associated to asymmetrical distributions. With the gamma distribution, a single parameter c (shape parameter) is enough to define a mathematical model of sunscreen distribution. The model was calibrated to calculate simulated SPFs similar to *in vivo* SPFs.[9] Wavelength by wavelength, inverse gamma distribution applied to Eq. (1) allowed a UV transmittance curve to form and thus to calculate a simulated SPF.

Simulated SPF is determined from the transmittance curve according to Eq. (2).

$$\text{Simulated SPF} = \frac{\int_{\lambda=290\ \mathrm{nm}}^{\lambda=400\ \mathrm{nm}} E(\lambda) \times I(\lambda) \times \mathrm{d}\lambda}{\int_{\lambda=290\ \mathrm{nm}}^{\lambda=400\ \mathrm{nm}} E(\lambda) \times I(\lambda) \times T(\lambda) \times \mathrm{d}\lambda}, \tag{2}$$

where $E(\lambda)$ is the erythema action spectrum (CIE-1987) at wavelenght λ; $I(\lambda)$ is the spectral irradiance received from the UV source at wavelength λ; $T(\lambda)$ is the mean monochromatic transmittance at wavelength λ.

2.3 *Protocol 1*

2.3.1 *Volunteers*

The present study was performed *in vivo* on six healthy volunteers, male and female, aged between 26 and 34 years. Approval had been obtained from the Ethics Committee of the Charité. The volunteers participating in the study had given their informed written consent.

The formulations were applied following the COLIPA protocol with 2 $\mathrm{mg/cm^2}$ on the forearms of the volunteers or the skin replica, respectively.

The homogeneity of distribution of the formulations on the skin was investigated by laser scanning microscopy, indirectly, before removal of tape strips and, directly, on the skin after 1 h, as after this penetration time the maximal homogeneity of the distribution of the sunscreen on the skin was certain. [14]

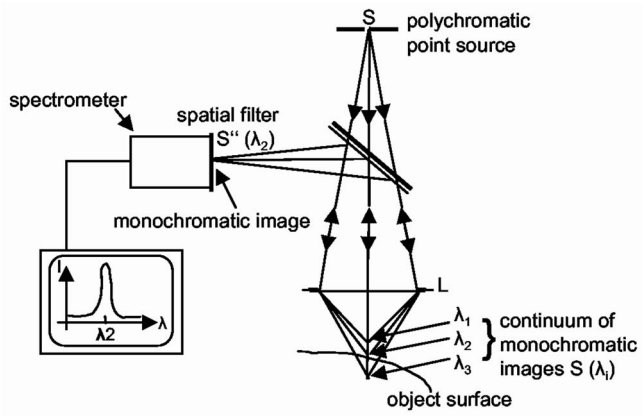

Fig. 1 Chromatic confocal setup for three-dimensional surface analysis.

2.3.2 *Tape stripping procedure*

The tape stripping procedure was performed, as described previously,[18,19] whereby, the skin was stripped using an adhesive tape (Tesa no. 5529, Beiersdorf, Hamburg, Germany). The tape strips were pressed onto the skin using a roller that stretches the skin surface and brings the tape strip in contact with the entire flat skin surface, which is normally structured by wrinkles and furrows. Then, the tape strips were removed with one quick movement.[20]

In the present investigation, one tape strip was removed from the sunscreen treated skin areas after a penetration time of 1 h. The tape strip was covered with corneocytes and the sunscreen formulation.

2.3.3 *Laser scanning microscopy*

The distribution of the formulations containing fluorescein on the removed tape strips was investigated utilizing laser scanning microscopy (LSM 2000, Carl Zeiss, Jena, Germany) with an excitation wavelength of 488 nm and a fluorescence wavelength of 600 nm.

Then, the same experiments were repeated *in vivo*. The distribution of the topically applied formulations was investigated utilizing a dermatological laser scanning microscope (LSM Stratum, OptiScan Ltd, Melbourne, Australia). Using this system, it was possible to investigate the sunscreen distribution directly on the living skin without taking tape strips.

2.4 *Protocol 2*

This protocol was performed using the chromatic confocal setup (Altisurf 500 station, Altimet, Thonon-les-Bains, France). The apparatus is able to analyze the microtopography and surface roughness without any contact. It is composed of an optical sensor, a motion controller, a *x*-*y* translation stage, and a microtopography software. A confocal optical sensor (Fig. 1) based on the white light chromatic aberration principle allows a high resolution: 10-nm vertical and 1-μm horizontal. Furthermore, the chromatic confocal setup exhibits the unique property of perfect focus depth of field, because at any given point of the chromatic axial field of view, there is only one wavelength perfectly focused, all the other wavelengths being absolutely inactive.

As a consequence, only an almost monochromatic light beam appears to focus onto the filtering pinhole (S'') that also acts as the entrance port of a spectrometer (Fig. 1). The central wavelength of this monochromatic light beam ($\lambda 2$) corresponds to the exact height of the measured object point. By electromechanical scanning of the object surface in the *x*-*y* direction, one can record the microtopographic structure of any type of surface without any contact.

Because of a relatively lengthy analysis time, measurements could not be carried out *in vivo* because of the movement of the volunteers. Therefore, replicas of the skin were prepared, which have the same microtopography as living skin.

2.4.1 *Skin replica*

Negative skin impression preparation. A skin image (50×50 mm^2) was realized with a medium consistency polyether impression material (ImpregumTMF, 3M ESPE, Seefeld, Germany).

The base paste (seven volumes) and catalyst dose (one volume) was stirred for approximately 45 s with a spatula.

After having obtained a uniform color, the mixture was applied onto the skin surface with the spatula. The thickness uniformity of the impression was obtained by softly applying a polymethylmethacrylate (PMMA) plate against the paste after application.

The negative skin impression could be unstuck after a drying time of approximately 10 min.

Positive skin impression preparation. The final skin impression (25×35 mm^2) was made with a mixture of 96% methyl methacrylate (Altuglas, Paris, France) and 4% catalyzer B (Altuglas, Paris, France).

The mixture was prepared in a glass cupel covered by an aluminium sheet. Subsequently, it was carefully applied onto the negative impression. In order to obtain the thinnest final skin impression possible, the liquid PMMA layer had to be flattened by a PMMA plate.

In order to be hardened and completely dried, the impression must be stocked at least 4 h under an extractor. After checking that it did not contain any cavities or bumps, the impression was removed from the mold.

2.4.2 *Analysis of thickness distribution of the formulations*

We applied 2 mg/cm^2 of sunscreen product in the form of a high number of small drops of equal volume and distributed it evenly over the entire skin replica surface by using a pipette. The sunscreen product was spread immediately over the entire surface using light strokes with a finger cot presaturated with the product. Spreading was completed as quickly as possible (less than 30 s). Then the sample was rubbed into the rough surface using strong pressure. This process took 20 to 30 s.

The sample thus obtained was allowed to settle for 15 min at room temperature to ensure a self-leveling of the formula.

The microtopography of the skin replica (about 7×6 mm^2) was analyzed before and after the distribution of the formulation. Then, both data were subtracted using mountain altimap software (ALTIMET, Thonon-les-Bains, France)

and the resulting FT distribution was calculated step by step from Eq. (2).

Product film microrelief

= skin replica microrelief with

product – skin replica microrelief without product (3)

3 Results

3.1 *Protocol 1*

According to protocol 1, the distribution of the topically applied sunscreen formulations were analyzed *ex vivo* on tape strips and *in vivo* on the skin surface utilizing laser scanning microscopy. The results of the analysis of the tape strips obtained immediately after the removal are shown in Fig. 2.

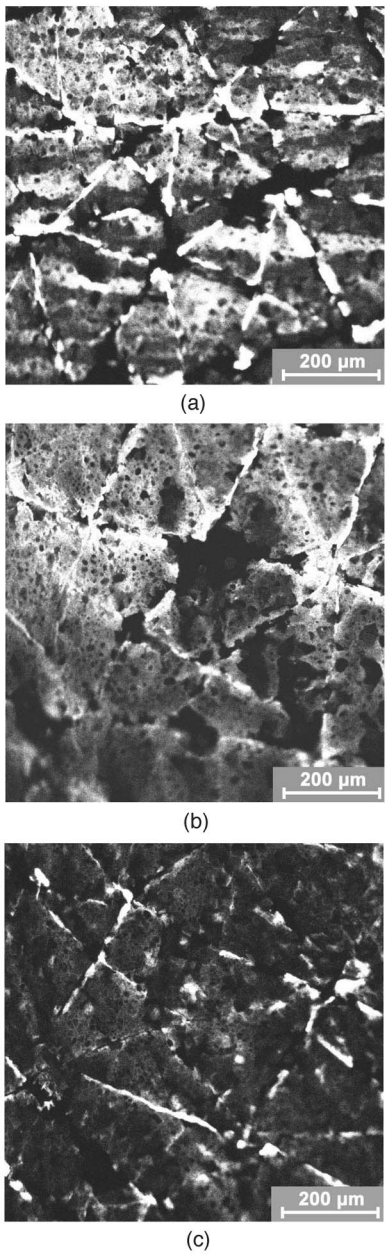

Fig. 2 Distribution of the dye containing formulations on the corneocytes removed by tape stripping (first tape strip): (a) formulation A; (b) formulation B; (c) formulation C.

The light areas represent the distribution of the fluorescein. The figures show that parts of the formulation are located in the furrows and wrinkles of the skin. In the case of formulations A and B, the corneocytes are better covered with the fluorescent formulation, as they appear lighter than in the case of formulation C. Here the highest amount of fluorescence is located in the furrows and wrinkles. The covering of the corneocytes, which appear as dark areas, is rather sparse.

Additionally, the distribution of the fluorescent dye, which represents a marker for the distribution of the sunscreen was determined *in vivo* to ensure that the *ex vivo* measurements reflect the real distribution of substances on the skin. The results of the *in vivo* measurements are presented in Fig. 3.

The *in vivo* measurements were carried out with a higher magnification than the *ex vivo* experiments utilizing the tape stripping technique. The figures show that the distribution on the living skin of the formulations A and B is more homogeneous, which is represented by a relatively homogeneous fluorescence than the distribution of formulation C. The formulations A and B cover the corneocytes to a larger extent, whereas, formulation C is located in the furrows of the skin. The *in vivo* results are in concordance with the *ex vivo* results obtained by analyzing the tape strips.

3.2 *Protocol 2*

Figures 4–6 represent the microrelief of the cream layer and the distribution of the cream thickness according to the three different vehicles.

Figure 4(a) shows that the sunscreen distribution on the skin replica of formulation A appears to be homogeneous. Only several small areas are not covered. Nevertheless, the surface of the upper corneocyte layer is well covered. Amounts of the formulation are also located in the furrows and wrinkles. The formulation microrelief can be quantitatively characterized, if one carries out a thresholding to evaluate the depleted sunscreen surface. A thresholding of 0.5 μm was chosen to represent a low thickness range: about 5 to 10% of the amount deposited, according to water evaporation.

Figure 4(b) represents the percentages of surface covered by different FT ranges $FT \leqslant 0.5\ \mu m$; $0.5\ \mu m < FT \leqslant 5\ \mu m$; $FT > 5\ \mu m$. The lowest height of cream (lower than 0.5 μm) calculated in red in Fig. 4(b), is primarily located on the high parts of the skin (i.e., the corneocytes). The percentage of surface covered by this low thickness, with cream inferior or equal to 0.5 μm represents 34% of the total area. This value will enable us to compare quantitatively the various products tested.

The sunscreen distribution of formulation B applied to the surface of the replica obtained from the same skin impression is represented in Fig. 5(a). The distribution seems similar to formulation A, but with an apparent slightly more homogeneous distribution of the cream. Also quantitatively, this formulation is similar to formulation A with a percentage of surface covered by a $FT \leqslant 0.5\ \mu m$ equal to 21%. In this case, also the amounts of cream are located in the wrinkles and furrows, as shown in Fig. 5(b).

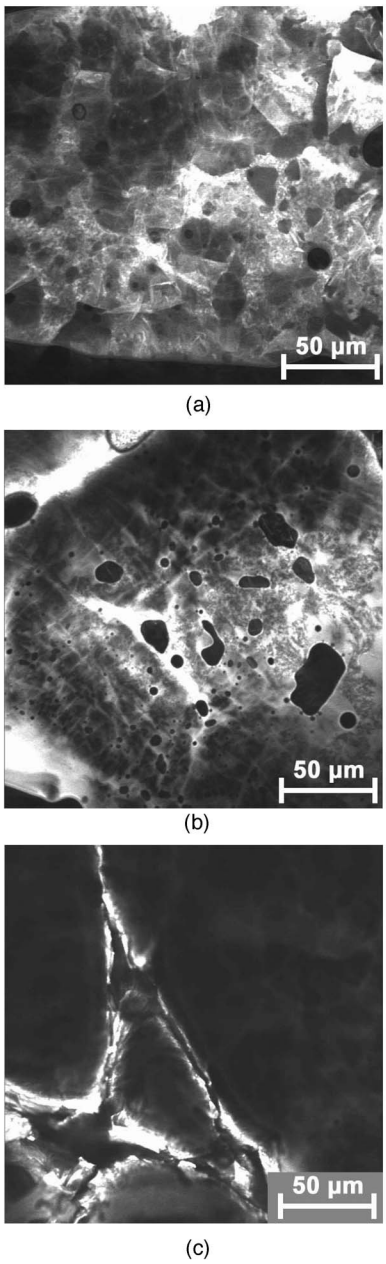

Fig. 3 Distribution of the dye containing formulations on the living skin measured by laser scanning microscopy: (a) formulation A; (b) formulation B; (c) formulation C.

The cream layer relief of formulation C is different from the two other formulations. In this case, Fig. 6(a) shows large areas of the skin surface with a very low amount of the product. The product is almost concentrated in the wrinkles and furrows of the replica. The distribution is less homogeneous than for products A and B. This observation is confirmed by the quantitative analysis [Fig. 6(b)]. Indeed, the percentage of surface covered by FT$\leqslant$0.5 μm is 48%, which is approximately double the value found in the case of the formula B.

Starting from the concentrations of the UV filters incorporated in each product, the calculation model, based on the gamma law distribution of an irregular sunscreen film,[9] allowed us to predict realistic SPFs. We simulated the theoretical SPF that one should obtain, if the three formulas were spread out as usual. The results obtained are represented in Table 1.

In the case of the good spreading formulas (A and B), the simulated and *in vivo* SPF are rather close (around 80%). On the other hand, these values are rather distant for product C with a less homogeneous distribution. *In vivo* value represents only 54% of the simulated value.

4 Discussion

The results of the present investigation showed that in all cases, the distribution of sunscreen formulations is more or less inhomogeneous. This has been indicated by both methods used. These findings are in concordance with previous investigations,[10,21,22] which revealed that topically applied substances do not distribute homogeneously on the skin. Furthermore, the measurements corresponding to protocol 1 again evidenced that the distribution of a sunscreen on removed tape strips reflects the current situation on living skin. Although it is important that the measurement is performed immediately after the removal of the tape strips, as in previous investigations, it has been shown that the distribution of topically applied substances on tape strips increases in homogeneity, eventually reaching an end point after 24 h, because of a diffusion of the substance into and inside the adhesive layer of the tape strip.[10]

The *in vivo* measurements using laser scanning microscopy directly on the skin indicated that after a penetration time of 1 h, the topically applied formulations are located particularly in the furrows and wrinkles of the skin. After a 1 h penetration time, the maximum homogeneity of the distribution of sunscreen formulations was achieved.[14] In the case of formulations A and B, the fluorescent dye, which represents a marker for the distribution of the UV filter, is also located around the corneocytes. Fluorescein can be used as a marker for the distribution of the sunscreen, as previous investigations have shown that penetration profiles of fluorescein and UV filter substances are approximately comparable. Advantages of both the *in vivo* and *ex vivo* laser scanning microscopy are that they represent complementary procedures that can be easily and quickly applied to determine the homogeneity of the distribution of sunscreens under realistic circumstances. Reproducible results can be obtained. Potential disadvantages of laser scanning microscopy are (1) expert eyes are helpful for the interpretation of the laser scan images, and (2) it represents a rather qualitative method. The distribution of a fluorescent dye, which represents the sunscreen, can be estimated visually. A distinction between inhomogeneous, increased homogeneous and homogeneous, can be clearly made, and a ranking of different products is feasible. However, if quantitative values are required, the possibility exists to determine the covering density, which has already been performed by Lindemann, et al.[23] who determined the density of the corneocytes on removed tape strips by laser scanning microscopy. Also the realization of protocol 2 of the present study revealed an inhomogeneity of the distribution of all investigated sunscreen formulations.

The utilization of the chromatic confocal setup offers several advantages:

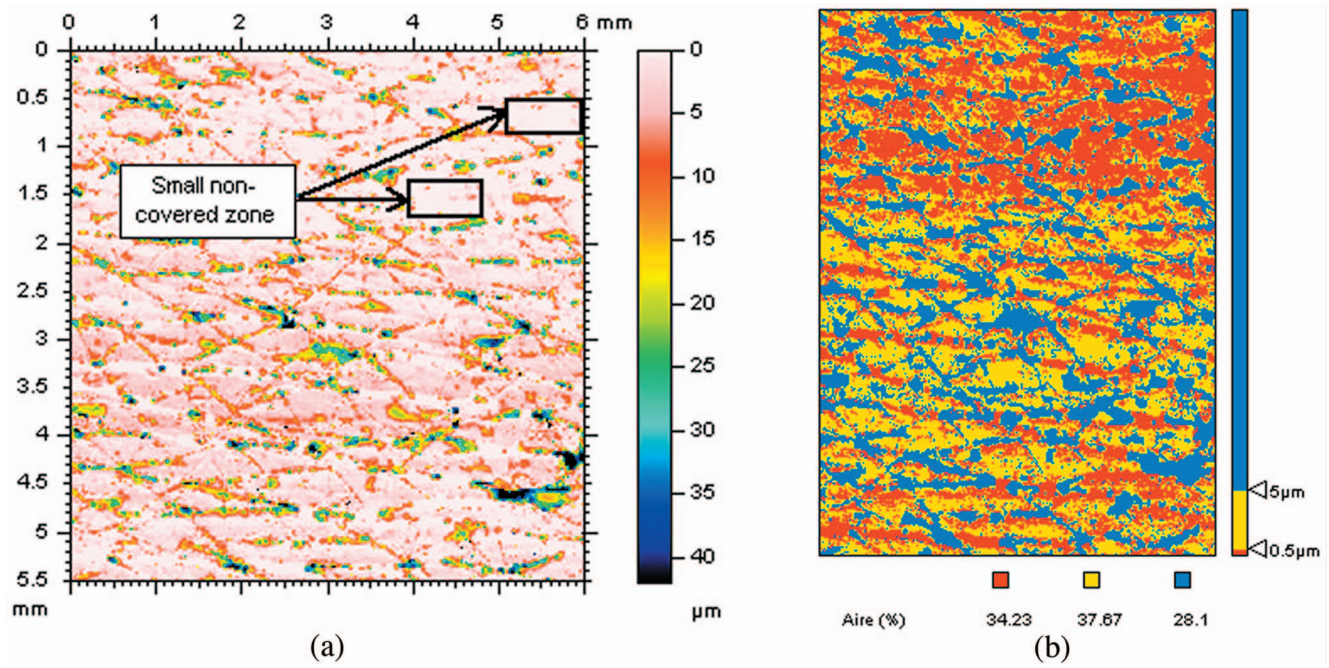

Fig. 4 Product A (a) cream layer relief [deduced from Eq. (1)], (b) percentage of surface covered by different FT ranges: FT$\leqslant$0.5 μm (red); 0.5 μm$<$FT$\leqslant$5 μm (yellow); FT$>$5 μm (blue).

• Chromatic perfect focus depth of field of 300 μm definitely avoids the z-axis scanning of the classical confocal scanning optical microscope. It also avoids the time-consuming computer reconstruction of the object image because at any given point on the scanned field the entire chromatic depth of field is "seen" at the same time.

• The irregular FT is very low in the depleted areas. Thus, the z-axis resolution must be submicronic. Other techniques like interference fringe profilometry present a resolution that is too low (5 μm) to be used.[24]

• It permits the determination of the microtopography of skin replica before and after the application of formulations without contact. A subtraction of both relief results in the formulation layer displays relief as a three-dimensional form.

• The appreciation of the distribution of the topically applied substance can be carried out visually by accounting the

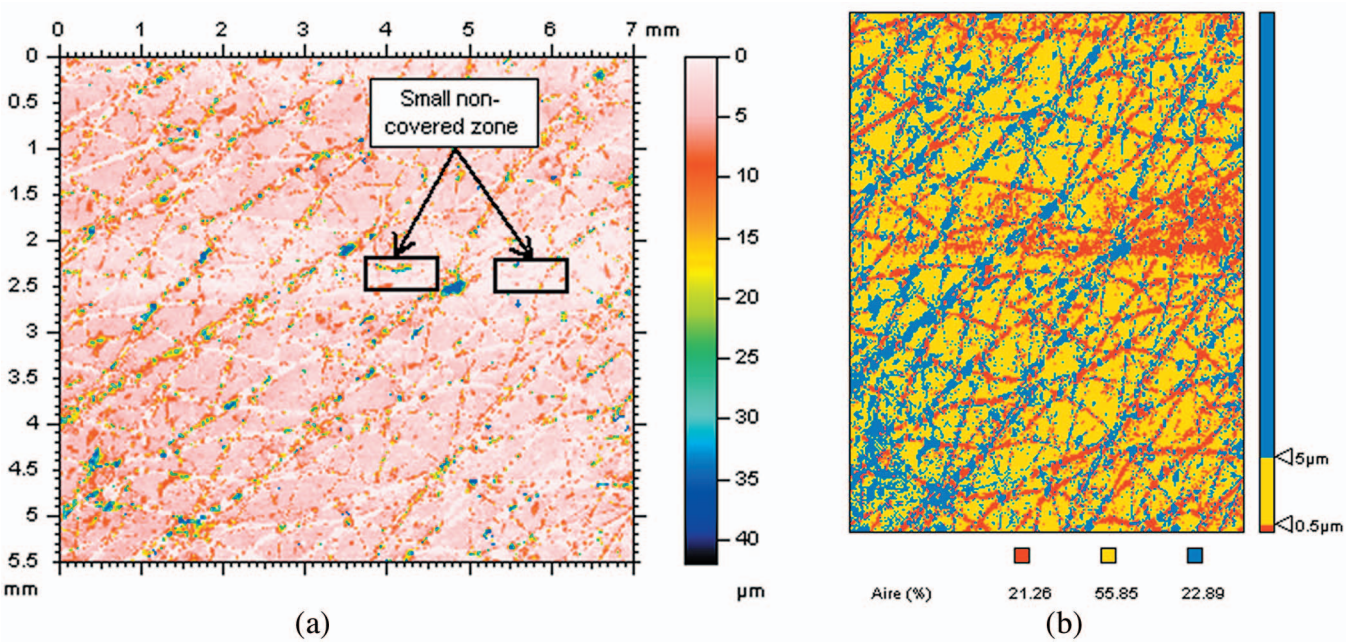

Fig. 5 Product B (a) cream layer [deduced from Eq. (1)] relief; (b) percentage of surface covered by different FT ranges: FT$\leqslant$0.5 μm (red); 0.5 μm$<$FT$\leqslant$5 μm (yellow); FT$>$5 μm (blue).

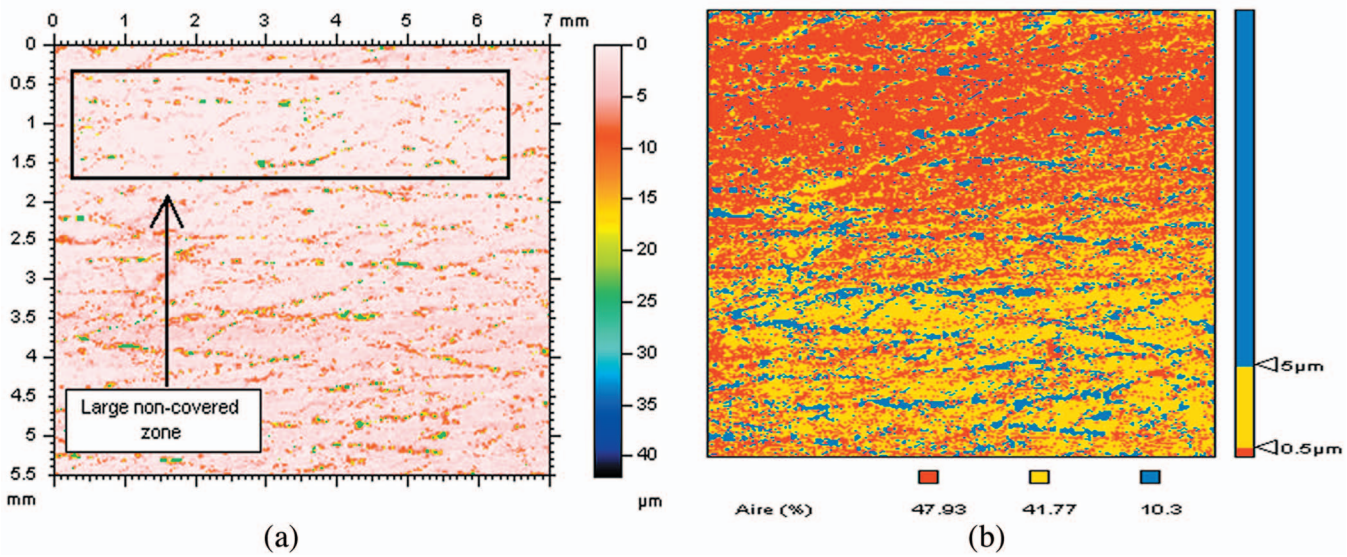

Fig. 6 Product C(a) cream layer relief [deduced from Eq. (1)]; (b) percentage of surface covered by different FT ranges: FT≤0.5 μm (red); 0.5 μm<FT≤5 μm (yellow); FT>5 μm (blue).

cream layer relief (qualitative method) and mathematically by calculating the percentages of cream heights (quantitative method). Significant percentages of low cream height indicate nonhomogeneous distribution. By utilizing this method, the comparison of percentage values is possible.

The chromatic confocal setup also has restrictions. This method, based on the determination of the microtopography before and after the application of formulations, imposes the use of a skin replica, because the relief of the skin must remain unchanged between two measurements. The use of living skin is impossible, as one cannot evaluate any effect depending on a skin chemical environment. Only skin microrelief is taken into account in this method.

The results of protocol 2 showed, like protocol 1, that the product repartition is different according to the vehicle.

Qualitatively, products A and B show a better homogeneous distribution than product C, as demonstrated in Fig. 4(a), 5(a), and 6(a). These results confirm the fact that the nonvolatile material content 30% for products A and B versus 18% for product C strongly influences homogeneity and thickness of the film left on the substrate.

In parallel, quantitative analysis showed a better covering of the skin replica in the cases of A and B (only 34% and 21% of the area, respectively, lower than 0.5 μm) than in the case of C (48% of the area lower than 0.5 μm). This is in concordance with the *in vivo* SPF of products A and B, representing around 80% of the simulated SPF, whereas, in the case of product C, it represents only 54%.

Table 1 Comparison of the simulated and *in vivo* SPF.

Product	Simulated SPF	*In Vivo* SPF	*In Vivo*/Simulated SPF
A	17	14±4	82%
B	14	11±3	79%
C	11	6±1	54%

The results of both protocols confirm that obviously a correlation between the ability to distribute homogeneously and the SPF exists. This is concordant with knowledge gained from spectroscopy, where it is well known that the disturbance of the homogeneous distribution reduces the intensity of the absorption. [9,14] Therefore, probably the choice of the vehicle already influences the efficacy of the UV filter.

5 Conclusion

The comparison of the methods utilized in this study showed that both methods represent suitable methods to determine the homogeneity of topically applied substances. It has been shown that the inhomogeneous distribution, which depends, on the one hand, on the structure of the skin and, on the other hand, on the spreading abilities of the vehicles used for the UV filters, has an influence on the SPF. In spite of differences in the chemical surface between a skin replica and living skin, the results seem to indicate that microrelief is the most important factor for the sunscreen distribution. Therefore, the determination of the homogeneity of the distribution of sunscreens on the skin should be a standard in sun protection research.

References

1. P. Elsner, S. Beissert, and T. A. Luger, "Lichtschutz: Möglichkeiten und grenzen," *J. Dtsch. Dermato. Ges.* **3**, 40–44 (2005).
2. H. I. M. Mahler, J. A. Kulik, J. Harrell, A. Correa, F. X. Gibbons, and M. Gerrarg, "Effects of UV photographs, photoaging information, and use of sunles stanning lotion on sun protection behaviours," *Arch. Dermatol.* **14**, 374 (2005).
3. H. C. Wulf, J. Sandby-Møller, T. Kobayasi, and R. Gniadecki, "Skin aging and natural photoprotection," *Micron* **35**, 185–191 (2004).
4. A. S. Turgay, D. Sari, M. Can, and R. E. Genc, "Determination of sunburn and skin cancer risk of outpatients in a dermatology polyclinic," *Asian Pac. J. Cancer Prev.* **6**(2), 143–146 (2005).
5. S. Grether-Beck, M. Wlaschek, J. Krutmann, and K. Scharffetter-Kochanek, "Photodamage and photoaging—Prevention and treatment.," *J. Dtsch. Dermatol. Ges.* **3**(2), 19–25 (2005).

6. M. Pissavini, L. Ferrero, A. Alard, U. Heinrich, H. Tronnier, D. Kockott, D. Lutz, V. Tournier, M. Zambonin, and M. Meloni, "Determination of the *in vitro* SPF," *Cosmet. Toiletries* **118**, 63-72 (2003).
7. L. Zastrow, L. Ferrero, T. Herrling, and N. Groth, "Integrated SPF: a new Sun Protection Factor based on Free Radicals generated by UV irradiation," *Skin Pharmacol. Physiol.* **17**, 219–231 (2004).
8. J. Schulz, H. Hohenberg, F. Pflücker, E. Gärtner, T. Will, S. Pfeiffer, R. Wepf, V. Wendel, H. Gers-Barlag, and K. P. Wittern, "Distribution of sunscreens on skin," *Ala. J. Med. Sci.* **54**(1), 157–163 (2002).
9. L. Ferrero, M. Pissavini, S. Marguerie, and L. Zastrow, "Efficiency of a continuous height distribution model of sunscreen film geometry to predict a realistic sun protection factor," *J. Cosmet. Sci.* **54**, 463–481 (2003).
10. H.-J. Weigmann, U. Jacobi, C. Antoniou, G. N. Tsikrikas, V. Wendel, C. Rapp, H. Gers-Barlag, W. Sterry, and J. Lademann, "Determination of penetration profiles of topically applied substances by means of tape stripping and optical spectroscopy: UV filter substances in sunscreens," *J. Biomed. Opt.* **10**(1), 14009 (2005).
11. J. J. O'Neill, "Effect of film irregularities on sunscreen efficacy," *J. Pharm. Sci.* **7**, 888–891 (1983).
12. P. M. Farr and B. L. Diffey, "How reliable are sunscreen protection factors?" *Br. J. Clin. Pract. Symp. Suppl.* **112**, 113–118 (1985).
13. R. M. Sayre, P. P. Agin, G. J. LeVee, and E. Marlowe, "A comparison of *in vivo* and *in vitro* testing of sunscreening formulas," *Photochem. Photobiol.* **29**(3), 559–566 (1979).
14. J. Lademann, A. Rudolph, U. Jacobi, H.-J. Weigmann, H. Schaefer, and W. Sterry, "Influence of nonhomogeneous distribution of topically applied UV filters on sun protection factors," *J. Biomed. Opt.* **9**(6), 1358–1362 (2004).
15. D. F. Tunstall, "A mathematical approach for the analysis of *in vitro* sun protection factor measurements," *J. Cosmet. Sci.* **51**, 303–315 (2000).
16. B. Herzog, "Prediction of sun protection factors by calculation of transmissions with a calibrated step film model," *J. Cosmet. Sci.* **53**, 11–26 (2002).
17. COLIPA "Sun protection factor test method," Ref. 94/289 (1994).
18. H.-J. Weigmann, J. Lademann, H. Meffert, H. Schaefer, and W. Sterry, "Determination of the horny layer profile by tape stripping in combination with optical spectroscopy in the visible range as a prerequisite to quantify percutaneous absorption," *Skin Pharmacol. Appl. Skin Physiol.* **12**, 34–45 (1999).
19. H.-J. Weigmann, J. Lademann, S. Schanzer, U. Lindemann, R. v. Pelchrzim, H. Schaefer, and W. Sterry, "Correlation of the local distribution of topically applied substances inside the stratum corneum determined by tape stripping to differences in bioavailability," *Skin Pharmacol. Appl. Skin Physiol.* **14**, 93–103 (2001).
20. J. Lademann, H.-J. Weigmann, S. Schanzer, H. Richter, H. Audring, C. Antoniou, G. Tsikrikas, H. Gers-Barlag, and W. Sterry, "Optical investigations to avoid the disturbing influences of furrows and wrinkles quantifying penetration of drugs and cosmetics into the skin by tape stripping," *J. Biomed. Opt.* **10**(5), 54015 (2005).
21. M. W. Brown, "The sun protection factor. Test methods and legal aspects," **2**, 10–18 (2002).
22. H. Piazena, "Phototherapie der Psoriasis," *Akt. Dermatol.* **27**, 255–261 (2001).
23. U. Lindemann, K. Wilken, H.-J. Weigmann, H. Schaefer, W. Sterry, and J. Lademann, "Quantification of the horny layer using tape stripping and microscopic techniques," *J. Biomed. Opt.* **8**(4), 601–607 (2003).
24. J. M. Lagarde, C. Rouvrais, D. Black, S. Diridollou, and Y. Gall, "Skin topography measurement by interference fringe projection: A technical validation," *Skin Res. Technol.* **7**, 112–121 (2001).